RESEARCH ARTICLE

Exploring the binding affinity and non-covalent interactions of anthocyanins with aging-related enzymes through molecular docking

John Sylvester B. Nas[1,2]

Author's email address: jbnas@up.edu.ph

[1]*Department of Biology, College of Arts and Sciences, University of the Philippines Manila, Ermita, Manila, 1000 Philippines*
[2]*Department of Medical Technology, Institute of Arts and Sciences, Far Eastern University Manila, Sampaloc, Manila, 1008 Philippines*

ABSTRACT

Background and Objective: Anthocyanins are associated with aging and longevity. However, the mechanism involving the pure anthocyanin compounds in aging remains elusive. To investigate the possible mechanism of action of the different anthocyanin compounds towards aging-associated enzymes, the lead-likeness, binding affinity, and binding interactions were evaluated.

Methodology: The different anthocyanin compounds such as cyanidin, delphinidin, malvidin, pelargonidin, peonidin, and petunidin were assessed for lead-likeness following the criteria of Lipinski's rule of five (Ro5). These same compounds were virtually docked to different aging-related enzymes involved in MAPK, AMPK, and insulin signaling pathways. The top binding anthocyanins for each enzyme were visualized and compared to the enzyme inhibitors.

Results: The different anthocyanin compounds abide with Ro5 denoting its potential as a lead compound. For each enzyme, there were different top-binding anthocyanins. The crystal structures of the docked anthocyanins reveal that there were different substructures involved during the non-covalent interaction. Some substructures, particularly the hydroxy groups, have different roles during the H-bond formation. These findings suggest that the various anthocyanin compounds may have a distinct mechanism of action towards a specific enzyme.

Conclusion: Taken together, these results suggest that the anthocyanin compounds may have varying effects in aging enzymes, which may be due to the differences in their substructures. Nonetheless, further investigations are needed to understand these findings using cells and animal models.

Keywords: *anthocyanin, aging, MAPK, AMPK, insulin signaling, in silico*

Introduction

Aging is commonly associated with various neurodegenerative diseases, cancer, and a weakened immune system [1,2]. Different age-related pathways are widely studied, such as mitogen-activated protein kinase (MAPK), AMP-activated protein kinase (AMPK), and insulin signaling pathways [3,4,5]. In MAPK pathway, mitogen-activated protein kinase-activated protein kinase 2 (MAPKAPK2), mitogen-activated protein kinase 10 (MAPK10), and B-raf kinase (B-raf) play essential roles during stress response [6,7]. Interesting enzymes in the AMPK pathway are sirtuin-3 (sirt3), sirtuin-6 (sirt6), and 5'-AMP-activated protein kinase catalytic subunit alpha-2 (AMPK2) earn recognition because of their role to regulate oxidative stress in diet restriction [8,9]. Meanwhile, three recognized enzymes in the insulin signaling pathway, namely insulin-like growth factor 1 receptor (IGF1R), phosphoinositide-dependent kinase-1 (PDK-1), and rac-alpha serine/threonine-specific kinase 1 (Akt1) affect development and reproductive aging as observed in various organisms [10,11,12].

Many studies associate crude anthocyanin extracts with these pathways through various model organisms, such as *Caenorhabditis elegans*, *Drosophila*, and mice, among others [13,14,15]. However, aging studies using pure compounds are limited to cyanidin, delphinidin, and peonidin [16,17,18].

Besides, the biological activities of the other pure anthocyanin compounds are not well understood.

Anthocyanin has six different classes, namely cyanidin, delphinidin, malvidin, pelargonidin, peonidin, and petunidin, as shown in Figure 1. These anthocyanins share the same aromatic rings, but they have different side chains. Delphinidin has the highest number of hydroxy groups with six, followed by cyanidin and petunidin with five. Meanwhile, the other anthocyanins only have four hydroxy groups. Some studies claim that the difference in the number of hydroxy groups affects their antioxidant potential [19,20]. Moreover, the amount of anthocyanin differs in a particular plant wherein some classes are dominant while some are absent [21]. These instances may give valid evidence to explain the biological activities of anthocyanins. Despite these evidences, only a few studies are using pure anthocyanin compounds, even though the crude anthocyanin has already been established association with aging. Most of the studies on pure compounds in aging investigated the effects of cyanidin and delphinidin [22,23].

To hypothesize a possible mechanism of action of the pure anthocyanin compound in aging, the researcher screened the anthocyanin compounds for lead-likeness, ranked their binding affinity with different aging-related enzymes, and compared the crystal structures of the docked top binding anthocyanin to the enzyme inhibitors.

Methodology

Data on the different classes of anthocyanins were from PubChem (www.pubchem.ncbi.nlm.nih.gov). The anthocyanins were namely cyanidin (CID: 128861), delphinidin (CID: 68245), malvidin (CID: 159287), pelargonidin (CID: 440832), peonidin (CID: 441773), and petunidin (CID: 441774). The aging-related enzymes MAPKAPK2 (PDB ID: 3A2C), MAPK10 (PDB ID: 1JNK), B-raf (PDB ID: 2FB8), SIRT3 (PDB ID: 3GLU), SIRT6 (PDB ID: 3PKI), AMPK2 (PDB ID: 3AQV),IGF1R (PDB ID: 1JQH), PDK-1 (PDB ID: 1OKY), and AKT1 (PDB ID: 3mv5) were downloaded from Protein Database (www.pdb.org). Known inhibitory ligands of these enzymes were identified through PDB and their information was downloaded, as well, from PubChem. Ligands affecting MAPK pathways related enzymes such as MAPKAPK2, MAPK10, and B-raf were n'-(4-ethoxyphenyl)-6-methyl-n-[(3S)-piperidin-3-yl]pyrazolo[1,5-a]pyrimidine-5,7-diamine (PDY) (CID: 49867482), phosphoaminophosphonic acid-adenylate ester (ANP) (CID: 33113); and (nz)-n-[5-[2-[4-[2-(dimethylamino)ethoxy]phenyl]-5-pyridin-4-yl-1h-imidazol-4-yl]-2,3-dihydroinden-1-ylidene]hydroxylamine (CID: 135398506), respectively [24,25,26]. Besides, known inhibitors of enzymes in AMPK pathway like SIRT3, SIRT6, and AMPK2 were adenosine-5-diphosphoribose (AR6) (CID: 447048) and dorsomorphin (TAK) (CID: 11524144), respectively [27,28,29]. Furthermore, enzymes involved in the insulin signaling pathway such as IGF1R, PDK-1, and Akt have known inhibitory

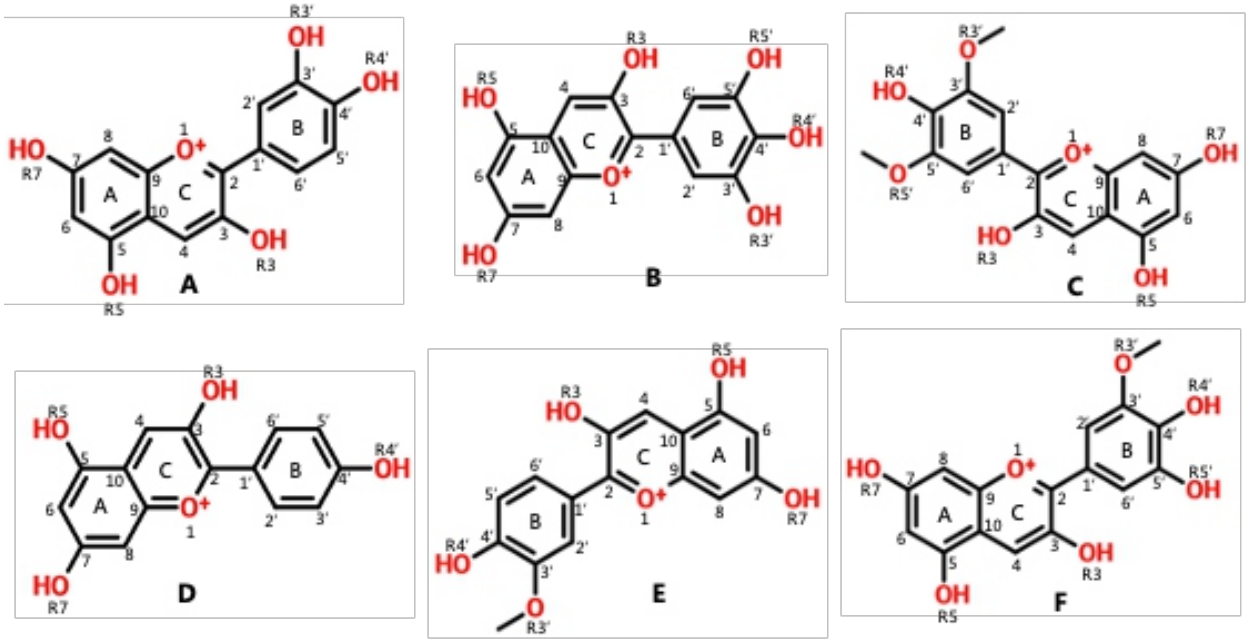

Figure 1. *The structure of the different anthocyanin compounds. A–cyanidin, B–delphinidin, C–malvidin, D–pelargonidin, E–peonidin, F–petunidin.*

ligands like phosphoaminophosphonic acid-adenylate ester (CID: 33113), staurosporine (CID: 44259), and (3R)-1-(5-methyl-7H-pyrrolo[2,3-d]pyrimidin-4-yl)pyrrolidin-3-amine (CID: 45480169), respectively [30,31,32].

Evaluation of the lead-likeness of the anthocyanin compounds

Data on the physicochemical properties of anthocyanin compounds and the known inhibitory ligands were collected from various databases such as PubChem, Mcule (Mcule Inc., USA), ChemAxon (www.chemaxon.com), and Chemmine Tools (www.chemminetools.ucr.edu). The different parameters such as mass, octanol/water partition coefficient (log P), H-bond acceptor, and H-bond donor were considered to assess the lead-like potential of the ligands following Lipinski's rule of five [33].

Virtual molecular docking of anthocyanin compounds

The different downloaded enzymes were prepared by adding hydrogens and Gasteiger charges. Then the charges were merged before removing non-polar hydrogen, lone pairs, water molecules, and non-standard residues as described in Mcule (Mcule Inc., USA) and Autodock Tools (version 1.5.6). The compounds were docked on the binding center of these enzymes, as follows: MAPKAPK2 (X: 21.9057, Y: 83.1144, Z: 115.101), MAPK10 (X: 22.4234, Y:11.9456, Z: 30.7271), B-raf (X: -16.755, Y: 4.9765, Z: -6.5064), sirt3 (X: 5.882, Y: -2.847, Z: 9.886), sirt6 (X: 6.3128, Y: -9.272, Z: 21.3634), AMPK2 (X: -7.8418, Y: 43.3926, Z: 7.0969), IGF1R (X: 6.5577, Y: 43.8166, Z: -7.3536), PDK-1 (X: 82.8551, Y: 18.3683, Z: 12.1003), and AKT-1 (X: 5.4361, Y: 3.1019, Z: 17.4783). The virtual screening predicted the binding affinity and orientation of the different classes of anthocyanin and known inhibitors with the target enzymes. Lastly, the most negative docking score was considered as the predicted free energy between the ligand and the receptor [34].

Visualization of the top-binding ligands and the inhibitory ligand of the aging-related enzymes

The interactions of the top-binding anthocyanin with the amino acid residues of the enzymes were visualized and compared with the enzyme inhibitor through PLIP (BIOTEC TU Dresden, Germany). The number of amino acid residue interacted, and the non-covalent interactions between the ligand and the receptors were characterized. The generated dock pose of the enzyme inhibitor in its respective enzyme was superimposed to the original structure in PDB to evaluate the validity of the docking experiment. The superimposition and the root mean square deviation of atomic position (RMSD) computation was done using Superpose v.1.0 (Wishart Lab, University of Alberta, Canada).

Results

Lead-likeness of different anthocyanin compounds and known inhibitory ligands

The six different classes of anthocyanin were assessed for their lead-likeness, as shown in Table 1. All the anthocyanin compounds, except delphinidin, have no Ro5 violation. The only violation delphinidin has is having greater than five H bond donors. Besides, one violation is still within the acceptable value, which denotes that all the anthocyanin compounds were lead.

In silico docking of different anthocyanin compounds to aging-related proteins

The different classes of anthocyanin underwent in silico docking to determine the possible aging-related enzyme it interacts. The binding energy (kcal/mol) measures the strength of the interaction between the ligand and the target enzyme, as shown in Table 2. Binding energies of the different anthocyanin compounds for enzymes related to MAPK pathways, such as MAPKAPK2, MAPK10, and B-raf are lower than the different known inhibitors PDY, ANP, and 215, respectively. The top-binding anthocyanin in the MAPK pathway differs in each enzyme, like delphinidin for MAPKAPK2, pelargonidin, and peonidin for MAPK10, and peonidin for B-raf. In the AMPK pathway, the binding energies of the anthocyanin compounds performed comparably well with AR6 and TAK, inhibitors of sirt3, and AMPK2, respectively. Conversely, their binding energy in MAPK10 is lower than the known inhibitor, AR6. The top-binding anthocyanin for sirt3, sirt6, and AMPK2 varies, namely delphinidin, petunidin, and peonidin, respectively. For the insulin signaling pathway, the binding energies of IGF1R and PDK-1 inhibitors, ANP and STU, were higher than the anthocyanin compounds. But XFE, Akt1 inhibitor, is comparable with the anthocyanin compounds. The top-binding anthocyanin compounds vary in each enzyme, such as delphinidin in IGF1R, malvidin and petunidin in PDK-1, and malvidin and petunidin in Akt1.

Evaluation of the binding interactions of the top-binding anthocyanin

The non-covalent interactions and the number of the interacting amino acid residue of the top binding

Table 1. *Lead-likeness of anthocyanin and various known ligands using Lipinski's Rule of Five*

Compounds	Mass	Log P	H bond acceptor	H bond donor	Ro5 violation
reference	≤500 g/mol	≤5	≤10	≤5	≤1
Cyanidin	287.24	2.9089	6	5	0
Delphinidin	338.69	-0.3815	7	6*	1
Malvidin	331.29	3.2205	7	4	0
Pelargonidin	271.24	3.2033	5	4	0
Peonidin	301.27	3.2119	6	4	0
Petunidin	317.26	2.9175	7	5	0

*Lipinski's rule of five violation, the number of H bond donor should be ≤5.

Table 2. *Ranking of the binding energies of the ligands in various aging-related enzymes*

MAPK Pathway			AMPK-related Pathway			Insulin Signaling Pathway		
MAPKAP2	MAPK10	BRAF	SIRT3	SIRT6	AMPK2	IGF1R	PDK-1	Akt1
PDY -7.3	ANP -9.0	215 -10.5	Delphinidin -9.3	AR6 -11.3	Peonidin -9.3	ANP -7.3	STU -8.8	Malvidin -8.3
Delphinidin -7.1	Pelargonidin -8.3	Peonidin -9.4	Pelargonidin -8.9	Petunidin -9.6	Cyanidin -9.2	Delphinidin -7.2	Cyanidin -8.7	Petunidin -8.3
Cyanidin -6.9	Peonidin -8.3	Cyanidin -9.3	Peonidin -8.8	Delphinidin -9.5	TAK -9.2	Petunidin -7.0	Pelargonidin -8.7	Delphinidin -8.0
Malvidin -6.9	Delphinidin -8.2	Malvidin -9.3	Petunidin -8.8	Cyanidin -9.3	Pelargonidin -9.2	Malvidin -6.9	Petunidin -8.6	Cyanidin -7.9
Petunidin -6.8	Malvidin -8.2	Pelargonidin -9.3	AR6 -8.6	Pelargonidin -9.3	Petunidin -9.0	Cyanidin -6.9	Delphinidin -8.5	Peonidin -7.9
Pelargonidin -6.8	Petunidin -8.2	Petunidin -9.3	Cyanidin -7.3	Peonidin -9.3	Delphinidin -8.8	Pelargonidin -6.8	Peonidin -8.4	Pelargonidin -7.6
Peonidin -6.8	Cyanidin -8.0	Delphinidin -9.2	Malvidin -5.5	Malvidin -9.2	Malvidin -8.8	Peonidin -6.8	Malvidin -8.2	XFE -7.1

anthocyanin compounds were evaluated and compared with the known inhibitor of the enzyme. To validate the docking experiment, the inhibitory ligands for the enzyme of interest were re-docked and compared with the original structure. All of the inhibitory enzymes have an overall RMSD value lower than 1.2 Å, which implies that the crystal structures of the re-docked ligand-enzyme are similar to the original [35]. Hence, the binding affinities in the molecular docking experiment were valid.

In MAPKAPK2, both PDY and delphinidin interact with the amino acids located in chain L (Figure 2). PDY (RMSD= 0.1 Å) has 4 hydrophobic interactions with val31, leu32, ala44, and leu 146. Also, PDY has H bonds in gln33 (2), leu94 (2), and glu98. Meanwhile, the delphinidin has 3 hydrophobic interactions in val31 (C2'), ala44 (C6), and leu 146 (C10). Besides, delphinidin forms H bonds with leu94 (R5), glu98 (R3'), and asp160 (R3). Both R5 and R3' were H bond acceptors, while R3 is the H bond donor. For their hydrophobic interactions in ala44, leu146, and val31, both of them bind to the same carbon atoms of ala44 and leu146 but in the different carbon atoms of val31. For their H bonding, both of them bonds with leu94 and glu98. However, PDY has 2 H bonds with leu94 and one of them has a similar donor atom with the H bond of delphinidin with leu94. Conversely, even though PDY and delphinidin have H bond with glu98, their donor atom from the MAPKAPK2 protein is different, N and O, respectively.

In MAPK10, ANP, pelargonidin, and peonidin show interaction with the amino acid in chain A (Figure 3). ANP (RMSD=0.1 Å) forms hydrogen bonds with ser28 (2), gln31, gly32, arg63, glu67, lys147, asn150, and asp 163, and a salt bridge with lys49. On the other hand, pelargonidin forms

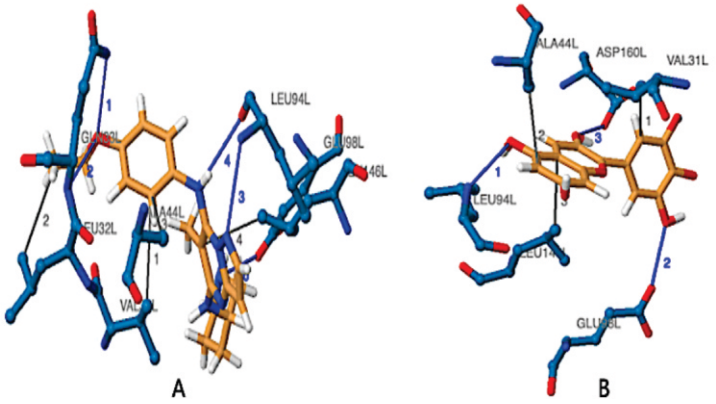

Figure 2. *Crystal structures of the ligands with MAPK2. A–PDY and B–delphinidin.*

hydrophobic interactions in gln31 (C4), val34 (C6'), lys49 (C6'), and leu162 (C5'). Pelargonidin has 6 hydrogen bonds with ala30 (R5), gln31 (R5), gly32 (R3), lys49 (O1), asn150 (R7), and asp163 (R7). Also, it forms a pi-cation interaction with lys49 (ring C). Similarly, peonidin and pelargonidin share the same hydrophobic interaction, H bond acceptors and pi-cation interactions, except that peonidin does not form H bond with gly32, which is an H bond donor. The hydrophobic interactions of pelargonidin and peonidin were on the same carbon atoms in the protein and their substructures, gln31, val34, lys49, and leu162. Meanwhile, the H bonds of pelargonidin and peonidin were on the same atoms in their substructures and the amino acids. ANP, pelargonidin, and peonidin form H bond with the same atoms in gln31, asn150, asp163.

In B-raf, 215 and peonidin interacts with the amino acids in chain B (Figure 4). The inhibitor 215 (RMSD=0.09 Å) has hydrophobic interactions in val23, lys35, thr81, and phe135 (2). Also, it forms H bonds with glu53, cys84, asp 146 (3), and phe147. Conversely, peonidin has hydrophobic interactions with val23 (2: C1', C2'), ile79 (C6), thr81 (C6), phe135 (C1'), and asp146 (C4). Besides, it forms H bonds with ala33 (R7), lys35 (R7), glu53 (R5), thr81 (2: R7), and asp146 (R3). Remarkably, R7 has two roles, which are a donor in ala33 and acceptor in lys35 and thr81. The inhibitor, 215, and the anthocyanin, peonidin, has the same hydrophobic interactions with val23, thr81, and phe135 on the same atoms of the amino acids. Meanwhile, they share H bonds with glu53 and asp146. Interestingly, in glu53, R5 atom in peonidin is the donor, while the O atom in 215 is the acceptor. This shows that the R5 atom in glu53 has a different role in these two ligands. In aspr146, the H bonds of peonidin and 215 involve different atoms of the amino acid.

In sirt3, the interactions of AR6 and delphinidin with the amino acids were visualized, as shown in Figure 5. AR6 (RMSD=0.79 Å) forms hydrogen bonds with 6 different amino acids, namely thr150, asp156, ser159, ser162(2), asn344, arg345, asp365, and val366. It also forms salt bridges with arg345. Contrastingly, delphinidin has hydrophobic interactions with asp156 (C8) and arg345 (C6'). Also, delphinidin forms H bond with 5 amino acids, such as ala146 (R7), thr150 (R3'), ser321 (R5), arg345 (5: R3x2, R3'x3), and val366 (R4'). Additionally, delphinidin has a pi-cation interaction with arg345 (ring B). AR6 and delphinidin have the same H bond formations with thr150, arg345, and val366 on the same atoms of the amino acids.

In sirt6, the docking of AR6 and petunidin on the amino acids found in chain A are shown in Figure 6. AR6 (RMSD=0.21 Å) forms H bond with 13 different amino acids, namely ala41, gly42, thr45 (2), phe52, arg53 (2), trp59, thr203, ser204 (3), asn228, leu229, gln230 (3), and val246. Also, it forms a salt bridge with arg53 (2). Conversely,

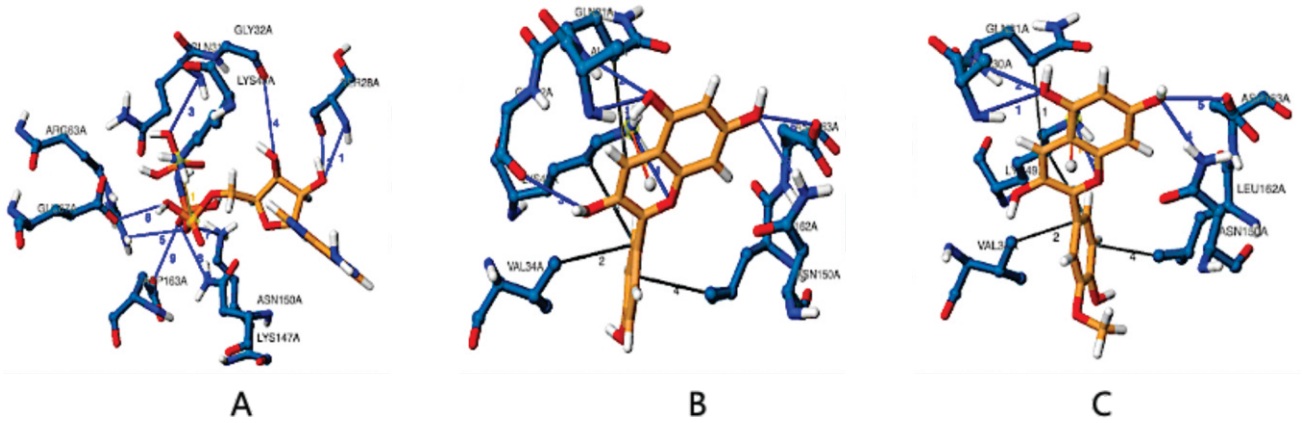

Figure 3. *Crystal structures of the ligands with MAPK10. A–ANP, B–pelargonidin, and C–peonidin.*

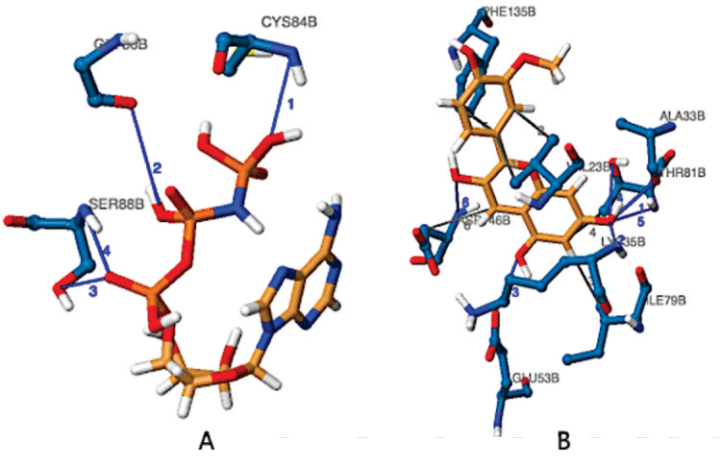

Figure 4. *Crystal structures of the ligands with B-raf. A–215 and B–peonidin.*

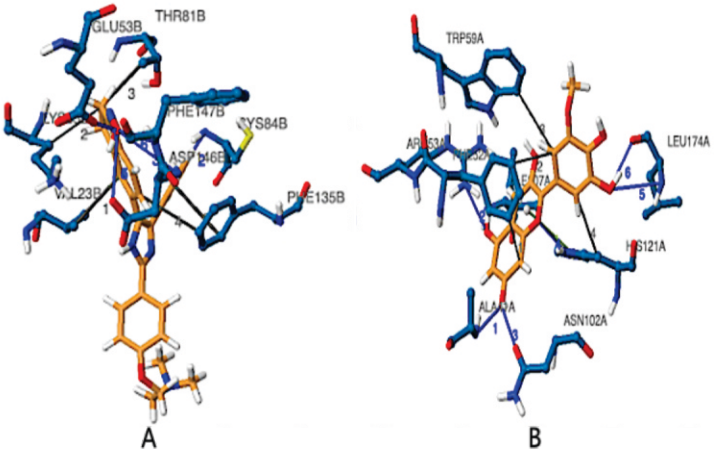

Figure 6. *Crystal structures of the ligands with sirt6. A–AR6 and B–petunidin.*

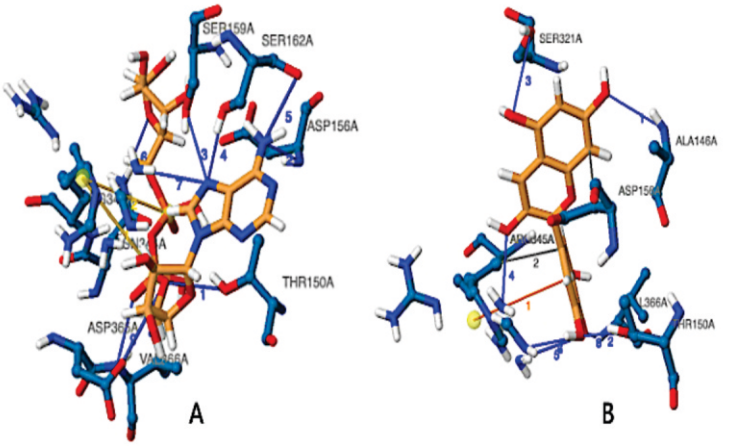

Figure 5. *Crystal structures of the ligands with sirt3. A–AR6 and B–pelargonidin.*

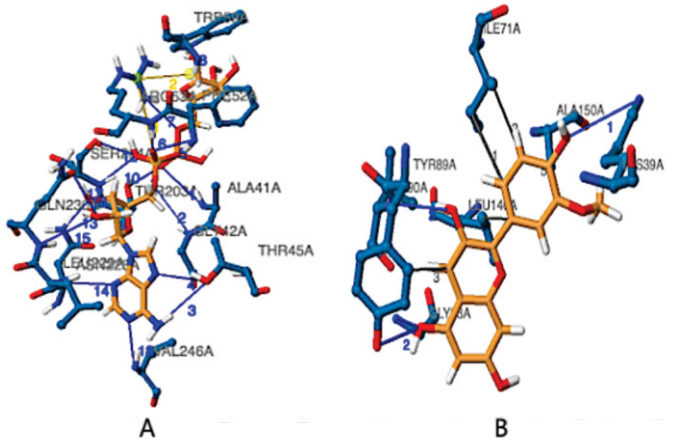

Figure 7. *Crystal structures of the ligands with AMPK2. A–TAK and B–cyanidin.*

petunidin has hydrophobic interactions with phe52 (2: C8 and C6'), trp59 (C6'), his121 (C2'), and ile207 (C4). It also has hydrogen bonds H bonds with only 5 different amino acids, such as ala41 (R7), arg53 (R5), asn102 (R7), his121 (O1), and leu174 (2: R3'x2). Additionally, petunidin has a pi-stacking with his121 (ring C). AR6 and petunidin formed H bonds on the same atoms of the amino acids ala41 and arg53.

In AMPK2, the dock posed of TAK and peonidin in the amino acids located in chain A is shown in Figure 7. TAK (RMSD=0.23 Å) has 9 hydrophobic interactions with different amino acids, particularly leu16, val24, ala37, ile71, asp97, tyr98, lys101, leu140, and ala150. Aside, it forms an H bond with val90. Meanwhile, the hydrophobic interactions of peonidin are in ile71 (2: C5' and C6'), tyr89 (C4), leu140 (C1'), and ala150 (C5'). Also, peonidin forms an H bond with lys39 (R3'), tyr89 (R5), val90 (R3), and gly93 (R5). All of these R groups are H bond acceptors, except for R5 with tyr89. Both TAK and peonidin have hydrophobic interactions with similar atoms in ile71, leu140, and ala150. Likewise, they formed an H bond in the same atom with val90.

In IGF1R, ANP and delphinidin are docked with amino acids of chain C, as shown in Figure 8. ANP (RMSD=0.31 Å) has H bonds with 4 amino acids, suchlike lys50, arg151, asp165 (3), and lys176. It also forms a salt bridge with lys50. On the contrary, delphinidin has hydrophobic interactions with leu22 (C6), ala48 (C6), and val80 (C4). It also forms H bonds with met99 (R5), asn152 (R5'), and asp165 (R3). R5 and R3 were H bond acceptors while R5' is an H bond donor. The H bond of delphinidin with asp165 shares similar atom with one of the H bonds of ANP in asp165.

In PDK-1, STU, cyanidin, and pelargonidin were visualized docked on the amino acids of chain A, as shown in Figure 9. STU (RMSD=0.11 Å) has hydrophobic interaction in

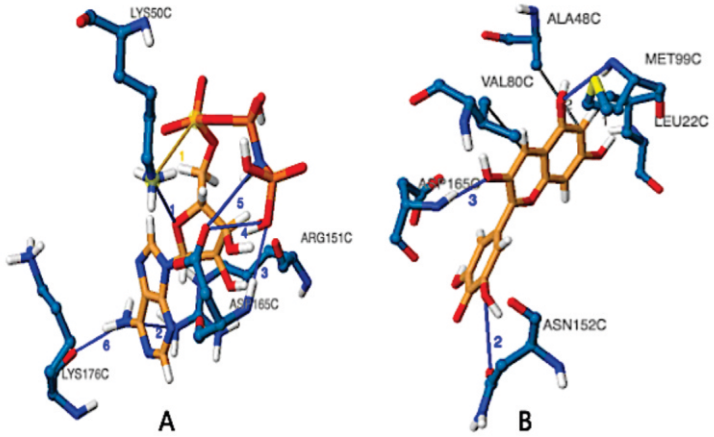

Figure 8. *Crystal structures of the ligands with IGF1R. A–ANP and B–delphinidin.*

five amino acids, specifically val25 (2), ala38, leu88, glu95, and leu141. It also forms hydrogen bonds with six amino acids, namely, glu19, ala91 (2), gly94, glu95, asn139, and asp152 (2). Cyanidin has hydrophobic interactions in leu17 (C3'), val25 (C10), leu88 (C4), phe22 (C6), ala38 (C6'), leu141 (C6'), and asp152 (C6). Meanwhile, the hydrophobic interactions of pelargonidin with leu 17 (2: C4 and C8), val25 (2: C2' and C3'), leu88 (C5'), tyr90 (C4), leu141 (C1'), and thr151 (C5'). The hydrophobic interactions of cyanidin and pelargonidin with leu17, val25, leu88, and leu49 all involve different atoms in their substructure. Meanwhile, cyanidin forms H bonds with lys40 (R5), ser89 (R5'), ala91 (2: R4' and R5'), asp152 (R5). R5' in ser89 and R4' in ala91 were H bond donors, while the rest were H bond acceptors. In pelargonidin, the H bond was formed with tyr90 (R5), ala91 (R3), lys92 (R5), gly94 (R5), thr151 (R4'). All of the amino acids were H bond donors, except for lys92. Both cyanidin and pelargonidin form H bond with ala91 in a different carbon atom. In cyanidin R4' is an H bond donor while R3 in pelargonidin is an H bond acceptor. Besides, STU, cyanidin, and pelargonidin also form H bond with ala91 in the same atom in the amino acid. Both pelargonidin and STU forms two hydrophobic interactions in the same atom of val25, while cyanidin has only one hydrophobic interaction but in a similar atom of val125. They also have similar hydrophobic interactions with the same atom of leu88 and leu141. STU and cyanidin have H bond but in different atoms in asp152. Meanwhile, STU and pelargonidin have an H bond with the same atom in gly94.

In Akt-1, XFE, petunidin, and malvidin interact with the amino acids in the A chain, as shown in Figure 10. Additionally, both malvidin and petunidin interact with the C chain of the enzyme. XFE (RMSD=1.18 Å) develops a hydrophobic interaction with thr148 and H bond with glu85 and ala87. Both malvidin and petunidin form a hydrophobic interaction with val21 (C6'), ala34 (C6), thr148 (C8), and phe295 (C4). Besides, malvidin forms H bond with arg4 (R4') in chain C and gly16 (R3'), glu85 (R7), ala87 (R5), and glu91 (R3) in chain A, where R7 and R3 were H bond donors. Petunidin develops an H bond with arg4 (R4') in chain C and leu13 (R3), gly16 (R5'), ala87 (R5), and asp149 (R3') in chain A, where R3 and R3' were H bond donors. Both petunidin and malvidin form H bonds in the same atoms with ala87 in A chain and arg4 in C chain, but different atoms with gly16. XFE, petunidin, and malvidin interact with the same atom in thr148, to develop the hydrophobic interactions. Similarly, they formed an H bond with ala87 in the same atom. However, only malvidin and XFE have the same atom acceptor in glu85. Moreover, petunidin and malvidin have the same atom acceptors in their H bond with arg4 and ala87.

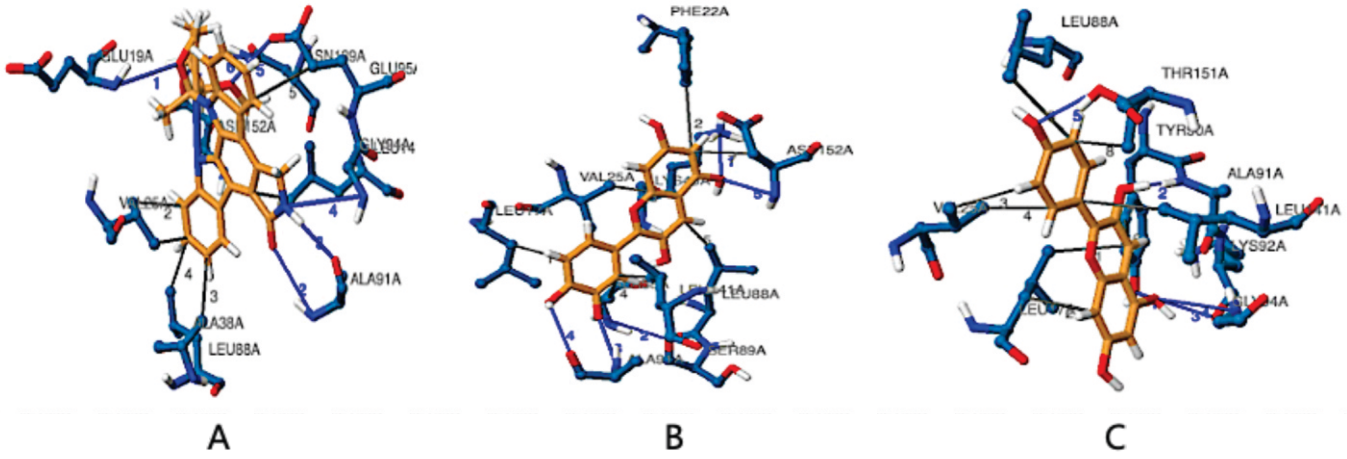

Figure 9. *Crystal structures of the ligands with PDK-1. A–STU, B–cyanidin, and C–pelargonidin.*

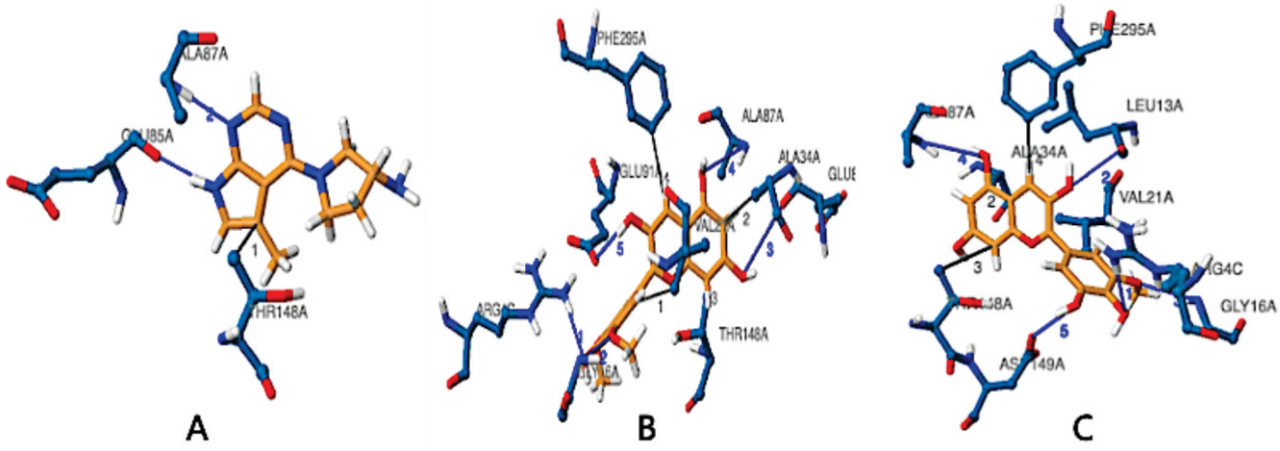

Figure 10. *Crystal structures of the ligands with Akt1. A–XFE, B–malvidin, and C–petunidin.*

Discussion

It is essential to consider the Absorption, Distribution, Metabolism, Elimination, and Transportation (ADMET) properties of a molecule to maintain its lead-likeness. The ADMET properties are affected by different factors such as molecular size, octanol/water partition coefficient (calculated log P), number of H bond acceptor, and number of H bond donors [36]. During the screening, delphinidin violated one of the rules in Lipinski's rule of five, which corresponds to greater than five H bond donors. More than five H bond donors may affect the permeation of the molecule through passive transport [37]. Some studies suggest the importance of the H bond donor-acceptor pairing mechanism in protein folding, which affects the receptor-ligand configuration [38]. Another study further explained that this instance happens because the interference of water molecules influences the binding affinity of a ligand with its receptor [39].

The physicochemical property of a compound may suggest its ADMET properties but not its affinity with an enzyme [40]. The docking score depicts the binding affinity of the ligand to the receptor [41]. The more negative the docking score is, the higher the binding affinity. The binding affinity of each anthocyanin to each target enzyme varies. To better explain the differences in their binding affinity, their binding interactions with the different enzymes were visualized.

In the MAPK pathway, delphinidin, pelargonidin, and peonidin were the top binding anthocyanin but failed to outrank the inhibitory ligands. After visualizing their interaction, the result shows that the inhibitors of MAPKAPK2, MAPK10, and B-raf relatively have high H bonding and roughly the same number of hydrophobic interactions compared with the anthocyanins. The greater the ability to form non-covalent interactions leads to the higher binding affinity of the known inhibitors with the proteins [42].

In the AMPK pathway, delphinidin and peonidin outranked the ligand inhibitors in sirt3 and AMPK2, but not in sirt6. The crystal structures of AR6 and delphinidin in sirt3 reveal that despite having about the same number of H bonds, delphinidin has a higher number of hydrophobic interactions. Also, the pi-cation interaction in delphinidin is stronger than the salt-bridge in AR6 [43]. Both salt-bridge and pi-cation interactions are associated with stabilizing the protein molecule [44,45]. There are reports that the stabilizing effect of salt-bridge in proteins varies [46,47,48]. These interactions may explain the stronger binding affinity of delphinidin compared to AR6. On the contrary, AR6 has a higher binding affinity compared to petunidin. Despite petunidin having hydrophobic interactions, the total number of non-covalent interactions in AR6 is greater. The high number of non-covalent interactions cover a large area of the protein. The force of interaction may have caused the surface area of the protein to minimize, which diminishes the movements inside the enzyme [49]. Conversely, TAK in AMPK2 has a lower binding affinity than peonidin, despite having a high number of hydrophobic interactions. Hydrophobic interactions are relatively stronger than the H bond [50]. In this finding, the hydrophobic interactions in peonidin may have been enhanced at the expense of the H-bonds [51].

In the insulin signaling pathway, the binding affinities of ANP and delphinidin with IGF1R, and the binding affinity of STU, cyanidin, and pelargonidin with PDK-1 were at par with

each other. This instance may be attributed to their similar numbers of non-covalent interactions. However, in Akt1, malvidin and petunidin have higher binding affinity than XFE, which may be due to the higher number of hydrophobic interactions and H bonds [42].

Overall, the anthocyanin compounds have a high binding affinity towards AMPK-associated enzymes, which may be due to the high number of hydrophobic interactions and H bonds formed with sirt3, sirt6, and AMPK2. Particularly, the anthocyanin compounds have a high binding affinity with sirt6. Remarkably, peonidin, which has a lower number of hydroxy groups compared with the other anthocyanins, also ranks the highest in the MAPK pathway but not in the insulin signaling pathway. In the insulin pathway, the top-binding anthocyanins vary in each enzyme. Malvidin, in particular, ranks the highest in Akt-1 but ranks the lowest in the other enzymes. One underlying explanation for these instances is the substructures of the anthocyanins involved during the non-covalent interactions, which vary in each enzyme. The common substructure of anthocyanins, which develops an hydrophobic interaction with the MAPK enzymes is C6, C6' for the AMPK enzymes, and C4 for insulin signaling enzymes. The high number of carbon atoms may favor hydrophobic interactions with the enzymes, which may result in a thermodynamic effect [52]. Meanwhile, the common substructure involved during H bond formations was R5 and R3 for MAPK, R3' and R5 for AMPK, and R3, R5, and R5' for the insulin signaling enzymes. Substructures R5, R3, R5', and R3' may have different roles, such as H bond donors, acceptors, or both at the same time. The hydroxy groups of the anthocyanin may have an impact on the H-bond formation with the enzyme [53]. These findings only suggest that the anthocyanin compounds may have different binding affinities with various aging-associated enzymes due to varying substructures that possibly affect their non-covalent binding interactions and binding affinities.

Conclusion

Anthocyanins are potential lead compounds for aging-associated enzymes. They have high affinity with enzymes in the AMPK pathway, but they exhibit diverse affinities in various enzymes. These variations may be associated with the varying identities and numbers of substructures involved in their non-covalent interactions, such as hydrophobic interaction, H bond formation, pi-cation interaction, and pi-stacking. It is of great interest to examine whether the effects of these variations are observable *in vitro* and *in vivo.*

References

1. Khansari N, Shakiba Y, Mahmoudi M. (2009) Chronic inflammation and oxidative stress as a major cause of age-related diseases and cancer. Recent Patents on Inflammation & Allergy Drug Discovery 3(1):73-80.
2. Licastro F, Candore G, Lio D, *et al.* (2005) Innate immunity and inflammation in ageing: A key for understanding age-related diseases. Immunity & Ageing 2(1):8.
3. Borrás C, Gambini J, Gómez-Cabrera MC, *et al.* (2005) 17β-oestradiol up-regulates longevity-related, antioxidant enzyme expression via the ERK1 and ERK2 [MAPK]/NFκB cascade. Aging Cell 4(3):113-118.
4. Greer EL, Brunet A. (2009) Different dietary restriction regimens extend lifespan by both independent and overlapping genetic pathways in *C. elegans*. Aging Cell 8(2):113-127.
5. Rincon M, Muzumdar R, Atzmon G, Barzilai N. (2004) The paradox of the insulin/IGF-1 signaling pathway in longevity. Mechanisms of ageing and development 125(6):397-403.
6. Davis T, Rokicki MJ, Bagley MC, Kipling D. (2013) The effect of small-molecule inhibition of MAPKAPK2 on cell ageing phenotypes of fibroblasts from human Werner syndrome. Chemistry Central Journal 7(1):18.
7. Papaconstantinou J, Hsieh CC. (2010) Activation of senescence and aging characteristics by mitochondrially generated ROS: How are they linked? Cell Cycle 9(19):3831-3833.
8. Qiu X, Brown K, Hirschey MD, Verdin E, Chen D. (2010) Calorie restriction reduces oxidative stress by SIRT3-mediated SOD2 activation. Cell metabolism 12(6):662-667.
9. Palacios OM, Carmona JJ, Michan S, *et al.* (2009) Diet and exercise signals regulate SIRT3 and activate AMPK and PGC-1α in skeletal muscle. Aging (Albany NY) 1(9):771.
10. Wang Y, Cheng Z, ElAlieh HZ, *et al.* (2011) IGF-1R signaling in chondrocytes modulates growth plate development by interacting with the PTHrP/Ihh pathway. Journal of Bone and Mineral Research 26(7):1437-1446.
11. Paradis S, Ailion M, Toker A, Thomas JH, Ruvkun G. (1999) A PDK1 homolog is necessary and sufficient to transduce AGE-1 PI3 kinase signals that regulate diapause in *Caenorhabditis elegans*. Genes & Development 13(11):1438-1452.

12. Wang SW, Cheung HP, Tong Y, *et al.* (2017) Steroidogenic effect of Erxian decoction for relieving menopause via the p-Akt/PKB pathway *in vitro* and *in vivo*. Journal of Ethnopharmacology 195:188-195.
13. Wang L, Li YM, Lei L, *et al.* (2015) Cranberry anthocyanin extract prolongs lifespan of fruit flies. Experimental Gerontology 69:189-195.
14. Yan F, Chen Y, Azat R, Zheng X. (2017) Mulberry anthocyanin extract ameliorates oxidative damage in HepG2 cells and prolongs the lifespan of *Caenorhabditis elegans* through MAPK and Nrf2 pathways. Oxidative Medicine and Cellular Longevity 2017.
15. Wu T, Yin J, Zhang G, Long H, Zheng X. (2016) Mulberry and cherry anthocyanin consumption prevents oxidative stress and inflammation in diet-induced obese mice. Molecular Nutrition & Food Research 60(3):687-694.
16. Meiers S, Kemény M, Weyand U, Gastpar R, von Angerer E, Marko D. (2001) The anthocyanidins cyanidin and delphinidin are potent inhibitors of the epidermal growth-factor receptor. Journal of Agricultural and Food Chemistry 49(2):958-962.
17. Chen PN, Chu SC, Chiou HL, Chiang CL, Yang SF, Hsieh YS. (2005) Cyanidin 3-glucoside and peonidin 3-glucoside inhibit tumor cell growth and induce apoptosis *in vitro* and suppress tumor growth *in vivo*. Nutrition and Cancer 53(2):232-243.
18. Nas JSB, Roxas CKF, Acero RRG, *et al.* (2019) *Solanum melongena* (Eggplant) Crude Anthocyanin Extract and Delphinidin-3-glucoside protects *Caenorhabditis elegans* against *Staphylococcus aureus* and *Klebsiella pneumoniae*. Philippine Journal of Health Research and Development 23(4):17-24.
19. Bajpai M, Pande A, Tewari SK, Prakash D. (2005) Phenolic contents and antioxidant activity of some food and medicinal plants. International Journal of Food Sciences and Nutrition 56(4):287-291.
20. Ichikawa H, Ichiyanagi T, Xu B, Yoshii Y, Nakajima M, Konishi T. (2001) Antioxidant activity of anthocyanin extract from purple black rice. Journal of Medicinal Food 4(4):211-218.
21. Zorenc Z, Veberic R, Stampar F, Koron D, Mikulic-Petkovsek M. (2016) Changes in berry quality of northern highbush blueberry (*Vaccinium corymbosum* L.) during the harvest season. Turkish Journal of Agriculture and Forestry 40(6):855-864.
22. Choi MJ, Kim BK, Park KY, Yokozawa T, Song YO, Cho EJ. (2010) Anti-aging effects of cyanidin under a stress-induced premature senescence cellular system. Biological and Pharmaceutical Bulletin 33(3):421-426.
23. Murata M, Kosaka R, Kurihara K, Yamashita S, Tachibana H. (2016) Delphinidin prevents disuse muscle atrophy and reduces stress-related gene expression. Bioscience, Biotechnology, and Biochemistry 80(8):1636-1640.
24. Fujino A, Fukushima K, Kubota T, Kosugi T, Takimoto-Kamimura M. (2013) Crystal structure of human cyclin-dependent kinase-2 complex with MK2 inhibitor TEI-I01800: Insight into the selectivity. Journal of Synchrotron Radiation 20(6):905-909.
25. Xie X, Gu Y, Fox T, *et al.* (1998) Crystal structure of JNK3: A kinase implicated in neuronal apoptosis. Structure 6(8):983-991.
26. King AJ, Patrick DR, Batorsky RS, *et al.* (2006) Demonstration of a genetic therapeutic index for tumors expressing oncogenic BRAF by the kinase inhibitor SB-590885. Cancer Research 66(23):11100-11105.
27. Jin L, Wei W, Jiang Y, *et al*. (2009) Crystal structures of human SIRT3 displaying substrate-induced conformational changes. Journal of Biological Chemistry 284(36):24394-24405.
28. Pan PW, Feldman JL, Devries MK, Dong A, Edwards AM, Denu JM. (2011) Structure and biochemical functions of SIRT6. Journal of Biological Chemistry 286(16):14575-14587.
29. Handa N, Takagi T, Saijo S, *et al*. (2011) Structural basis for compound C inhibition of the human AMP-activated protein kinase α2 subunit kinase domain. Acta Crystallographica Section D: Biological Crystallography 67(5):480-487.
30. Pautsch A, Zoephel A, Ahorn H, Spevak W, Hauptmann R, Nar H. (2001) Crystal structure of bisphosphorylated IGF-1 receptor kinase: Insight into domain movements upon kinase activation. Structure 9(10):955-965.
31. Komander D, Kular GS, Bain J, Elliott M, Alessi DR, Van Aalten DM. (2003) Structural basis for UCN-01 (7-hydroxystaurosporine) specificity and PDK1 (3-phosphoinositide-dependent protein kinase-1) inhibition. Biochemical Journal 375(2):255-262.
32. Freeman-Cook KD, Autry C, Borzillo G, *et al*. (2010) Design of selective, ATP-competitive inhibitors of Akt. Journal of medicinal chemistry 53(12):4615-4622.
33. Nogara PA, Saraiva RDA, Caeran Bueno D, *et al*. (2015) Virtual screening of acetylcholinesterase inhibitors using the Lipinski's rule of five and ZINC databank. BioMed Research International 2015.

34. Mobley DL, Graves AP, Chodera JD, McReynolds AC, Shoichet BK, Dill KA. (2007) Predicting absolute ligand binding free energies to a simple model site. Journal of Molecular Biology 371(4):1118-1134.
35. Kufareva I, Abagyan R. (2012) Methods of protein structure comparison. In: Orry A, Abagyan R (eds.). Homology Modeling: Methods and Protocols, New Jersey: Humana Press, pp. 231-257.
36. Lipinski CA, Lombardo F, Dominy BW, Feeney PJ. (1997) Experimental and computational approaches to estimate solubility and permeability in drug discovery and development settings. Advanced Drug Delivery Reviews 23(1-3):3-25.
37. Benet LZ, Hosey CM, Ursu O, Oprea TI. (2016) BDDCS, the rule of 5 and drugability. Advanced Drug Delivery Reviews 101:89-98.
38. Gao S, Wu W, Mo Y. (2009) The B− H··· H− P dihydrogen bonding in ion pair complexes [(CF3) 3BH−][HPH3− n (Me) n+](n= 0− 3) and its implication in H2 elimination and activation reactions. The Journal of Physical Chemistry A 113(28):8108-8117.
39. Chen D, Oezguen N, Urvil P, Ferguson C, Dann SM, Savidge TC. (2016) Regulation of protein-ligand binding affinity by hydrogen bond pairing. Science Advances 2(3) e1501240.
40. Korkuć P, Walther D. (2015) Physicochemical characteristics of structurally determined metabolite-protein and drug-protein binding events with respect to binding specificity. Frontiers in Molecular Biosciences 2:51.
41. Copeland RA. (2013) Evaluation of enzyme inhibitors in drug discovery: A guide for medicinal chemists and pharmacologists. New Jersey: John Wiley & Sons.
42. Klebe G. (2015) Protein-ligand interactions as the basis for drug action. In: Scapin G, Arnold E, Patel D. (eds.). Multifaceted Roles of Crystallography in Modern Drug Discovery, Dordrecht: Springer, pp. 83-92.
43. Gallivan JP, Dougherty DA. (2000) A computational study of cation− π interactions vs salt bridges in aqueous media: Implications for protein engineering. Journal of the American Chemical Society 122(5):870-874.
44. Petersen FN, Jensen MØ, Nielsen CH. (2005) Interfacial tryptophan residues: A role for the cation-π effect? Biophysical Journal 89(6):3985-3996.
45. Kumar S, Nussinov R. (1999) Salt bridge stability in monomeric proteins. Journal of Molecular Biology 293(5):1241-1255.
46. Barril X, Aleman C, Orozco M, Luque FJ. (1998) Salt bridge interactions: Stability of the ionic and neutral complexes in the gas phase, in solution, and in proteins. Proteins: Structure, Function, and Bioinformatics 32(1):67-79.
47. Waldburger CD, Schildbach JF, Sauer RT. (1995) Are buried salt bridges important for protein stability and conformational specificity? Nature Structural Biology 2(2):122-128.
48. Waldburger CD, Jonsson T, Sauer RT. (1996) Barriers to protein folding: Formation of buried polar interactions is a slow step in acquisition of structure. Proceedings of the National Academy of Sciences 93(7):2629-2634.
49. Williams DH, Stephens E, O'Brien DP, Zhou M. (2004) Understanding noncovalent interactions: Ligand binding energy and catalytic efficiency from ligand-induced reductions in motion within receptors and enzymes. Angewandte Chemie International Edition 43(48):6596-6616.
50. Chang, R. (2005) Physical chemistry for the biosciences. Sausalito, CA: Edwards Brothers, Inc. pp. 508-510.
51. Patil R, Das S, Stanley A, Yadav L, Sudhakar A, Varma AK. (2010) Optimized hydrophobic interactions and hydrogen bonding at the target-ligand interface leads the pathways of drug-designing. PloS one 5(8) e12029.
52. Xiao J, Cao H, Wang Y, Yamamoto K, Wei X. (2010) Structure–affinity relationship of flavones on binding to serum albumins: Effect of hydroxyl groups on ring A. Molecular Nutrition & Food Research 54(S2):S253-S260.
53. Myslinski JM, Clements JH, DeLorbe JE, Martin SF. (2013) Protein–ligand interactions: Thermodynamic effects associated with increasing the length of an alkyl chain. ACS Medicinal Chemistry Letters 4(11):1048-1053.